Journal of Statistical Physics, Vol. 72, Nos. 1/2, 1993

A New Transition for Projections of Multifractal Measures and Random Maps

Günter Radons[1]

Received December 31, 1992

Typical projections of simple multifractal measures with generalized dimensions D_q onto subspaces of dimension D are considered. It is known that for $D_0 > D$ almost all projections have Euclidean support. Here it is shown that if in addition D_∞ increases beyond D, a typical projection changes from a singular continuous distribution to an absolutely continuous measure with a square-integrable, or even differentiable density, and thus from a multifractal to an ordinary distribution with trivial singularity spectrum. Since projections of strictly self-similar measures can be regarded as invariant distributions of iterated function systems, such a transition is found also there and is expected to occur in related systems.

KEY WORDS: Multifractals; random maps; invariant measure; iterated function systems.

1. INTRODUCTION

Multifractals and multifractal spectra have proven to be important concepts in many areas of physics,[1-8] such as nonlinear dynamics, growth processes, turbulence, etc. In applications it may happen that for some reason one is able to observe only projections of a multifractal distribution, i.e., only integrals over some coordinates or degrees of freedom are available. Fundamental questions are then: What can we learn from a projection about the original multifractal, or what are the characteristics of projected multifractals? Are they again multifractal distributions or not? These problems are addressed in the present paper.

A closely related question concerns the nature of invariant distributions of iterated function systems.[9] Such systems, which are obtained by

[1] Institut für Theoretische Physik, Universität Kiel, D-24118 Kiel, Germany.

0022-4715/93/0700-0227$07.00/0

randomly composing linear maps, may be used for the construction of fractals and for image processing,[9] and in their nonlinear versions they occur in many branches of physics and science: We mention random Ising models,[10] versions of the Anderson model,[11] chaotic repellers in dynamical systems,[5] neural networks,[12] mathematical learning models,[13] and certain prediction problems.[14] The results given below are also relevant for these systems.

The content of this paper is organized as follows: In Section 2 we state the main results and subsequently show their validity for projections from the plane onto lines. This is done first for products of one-dimensional multifractal measures, where a rigorous treatment is possible, and then we give a heuristic explanation which shows the generality of the results. In Section 3 we establish the connection with invariant densities of certain iterated maps. A proof for projections from arbitrary dimensions onto hyperplanes of some lower dimensions is given in the Appendix. As illustration we consider products of strictly self-similar measures of Cantor type with unequal probabilities, for which the generalized dimensions or the singularity spectrum are known analytically.

2. RESULTS

The main results of this paper are that there are three distinct possible cases with respect to the nature of projected multifractal distributions:

1. SC-F: A typical orthogonal projection of a multifractal with fractal support results again in a multifractal with fractal support (SC-F: singular continuous with fractal support).
2. SC-E: The projected distribution is again a multifractal, but it has Euclidean support, i.e., its fractal dimension is an integer (SC-E: singular continuous with Euclidean support).
3. AC: The projection results in a ordinary, square-integrable density and is therefore no multifractal at all (AC: absolutely continuous).

The first case, SC-F, occurs whenever D_0, the fractal dimension of the original multifractal is smaller than D, the dimension of the space on which one projects. This is just the application of a result by Mattila[15] to the support of singular distributions. It also implies that one has $D_0^{(N,D)} = D_0$, where $D_0^{(N,D)}$ denotes the fractal dimension of the distribution obtained by projecting a multifractal with Euclidean dimension N onto D-dimensional hyperplanes.

In both cases SC-E and AC we have accordingly $D_0 > D$ and $D_0^{(N,D)} = D$. The distinction between cases SC-E and AC is new and depends on

the ratio of the generalized dimension[1] $D_\infty = D(q=\infty)$ of the original multifractal and D: For $D_\infty/D<1$ we have case SC-E, otherwise case AC.

First we will show under which conditions projections of multifractal product measures have a square-integrable density. This is particularly simple in the case of projections from R^2 onto lines. The arguments will be given here in detail, since the reasoning in higher dimensions follows along similar lines. Denote by $\hat{n}=(n_1, n_2)$ a unit vector parallel to the line onto which we project, i.e., we integrate over lines perpendicular to $\hat{n}$. An orthogonal projection $\rho_p(\xi)$ of a density $\rho(\mathbf{x})$ in R^2 can be expressed as

$$\rho_p(\xi)=\int d^2x\, \delta(\xi-\hat{n}\mathbf{x})\, \rho(\mathbf{x}) \tag{1}$$

It is easily seen that the Fourier transform $\hat{\rho}_p(k)$ of the projected density can be expressed as

$$\hat{\rho}_p(k, \hat{n})=\hat{\rho}_1(n_1 k)\cdot\hat{\rho}_2(n_2 k) \tag{2}$$

where the $\hat{\rho}_i$ are the Fourier transforms of the factors of the density $\rho(\mathbf{x})$. For multifractal densities which are mathematically not well defined, the $\hat{\rho}_i$ have to be interpreted as Fourier–Stieltjes transforms of the corresponding measures $\hat{\rho}_i=\int e^{ikx}\, d\mu_i(x)$. The integrated densities $\mu_i(x)$ form devil's staircases in the case of Cantor measures.

A projection has a square-integrable density $\rho_p(\xi)$ if $\int \rho_p^2(\xi)\, d\xi = (2\pi)^{-1}\int |\hat{\rho}_p(k)|^2\, dk$ is finite. Note that by definition a projection along one of the coordinate axes recovers one of the factors of the product measure, which are required to be singular, and so the integral always diverges for these directions, e.g., for $\hat{n}=(1, 0)$. Thus the most one can expect is to find parameter regions where almost all projections lead to a square-integrable $\rho_p(\xi)$. The latter is the case if $\int_c d\mathbf{n}\int dk\, |\hat{\rho}_p(k, \mathbf{n})|^2<\infty$, where the contour C is a (half) unit circle in $\mathbf{n}$ space. The proof of square-integrability, however, is simpler and generalizes easier to arbitrary dimensions if one instead integrates over a full unit square at the origin of $\mathbf{n}$ space, i.e., over a continuum of equivalent contours. In addition with no loss of generality we can restrict the $\mathbf{n}$ integration and the k integral to positive values. Thus we consider

$$I=\int_0^1 dn_1 \int_0^1 dn_2 \int_0^\infty dk\, |\hat{\rho}_1(n_1 k)|^2\cdot|\hat{\rho}^2(n_2 k)|^2 \tag{3}$$

which is equal to

$$\int_0^\infty dk\, k^{-2}\varphi_1(k)\cdot\varphi_2(k) \tag{4}$$

where we defined $\varphi_j(k) = \int_0^k |\hat{\rho}_j(k')|^2 \, dk'$. It is known[16] that $\varphi_j(k) = O(k^{1-\alpha_j})$, where α_j is the Lipshitz–Hölder exponent of the measure $\mu_j(x)$, which in the multifractal literature is known as $\alpha_{\min}$ and which we therefore denote as $\alpha^{(1)}_{\min,j}$ to indicate dimension and index of the factors. The integral (4) converges if the integrand decays faster than k^{-1} for $k \to \infty$, which leads to the condition $\sum_{j=1}^{2} \alpha^{(1)}_{\min,j} > 1$. Since we are considering product measures, this sum is equal to $\alpha^{(2)}_{\min} = D^{(2)}_{\infty}$, the minimal scaling index, respectively generalized dimension $D(q = \infty)$, of the original 2-dimensional multifractal.[1-8]

In order to understand these results and also its generality, consider the product of two equal triadic Cantor measures, where each is obtained by iteratively dividing intervals into two subintervals with length ratio $a \leqslant 1/2$ (e.g., $a = 1/3$ for the standard triadic Cantor set) and distributing "mass" to the subintervals with the ratios p and $1-p$, respectively, where p is the larger mass ratio, i.e., $1/2 \leqslant p \leqslant 1$. The most divergent contribution in the iterative construction of the singular 2D density comes from squares where the density grows in each step by a factor p^2/a^2, i.e., $\rho_n^{(2)} \sim a^{n(\alpha^{(2)}_{\min} - 2)}$ with $D^{(2)}_{\infty} = \alpha^{(2)}_{\min} = 2 \ln p / \ln a = 2\alpha^{(1)}_{\min} \leqslant 2$, where $D^{(N)}_q$ and $\alpha^{(N)}_{\min}$ denote also in the following the generalized dimension and minimal scaling index of a multifractal with Euclidean dimension N.[1-8] In a projection, however, the density corresponding to these squares $\rho_n^{(2,1)}$ grows only by a factor p^2/a in each iteative step and therefore $\rho_n^{(2,1)} \sim a^{n(\alpha^{(2)}_{\min} - 1)}$, which is divergent for $n \to \infty$ only if $\alpha^{(2)}_{\min} < 1$. This explains the result of the proof given above: If we have $\alpha^{(2)}_{\min} = D^{(2)}_{\infty} > 1$ the contribution of each square to the density approaches zero for $n \to \infty$, and if there is no systematic buildup of densities from individual squares which sum up in a projection, the projected density remains bounded and therefore square-integrable. There are exceptions, like the projections along the axes, where one recovers one of the factors of the product measure and thus gets divergent densities: Summing up individually vanishing densities can also result in a divergence of the sum at certain coordinates in the projection. The boundedness of integral I of Eq. (3) for $D^{(2)}_{\infty} > 1$ shows, however, that these exceptions are of measure zero with respect to all possible projections.

The above reasoning implies, on the other hand, that a projection leads to a singular continuous measure if $\alpha^{(2)}_{\min} = D^{(2)}_{\infty} < 1$ since all the fractal subsets of the 2D multifractal with singularity exponents[3] α with $\alpha^{(2)}_{\min} < \alpha < 1$ "survive" the projection in the sense that these lead to a divergent multifractal density also in the projection. This allows for two distinct situations with either the fractal dimension $D^{(2)}_0 > 1$ or $D^{(2)}_0 < 1$, which leads in the former case to a distribution with Euclidean support, i.e., $D^{(2,1)}_0 = 1$ (SC-E) and in the latter to a distribution with fractal support $D^{(2,1)}_0 = D^{(2)}_0$ (SC-F). In both cases the projection is a "true" multifractal

with a nontrivial multifractal $f(\alpha)$ spectrum.[3] In contrast, for $D_\infty^{(2)} > 1$ the $f(\alpha)$ spectrum of a projected distribution is trivial since it reflects just the power law behavior at the boundary points of the distribution.

To illustrate these results, consider the product of two equal Cantor measures as defined above. This 2D distribution is characterized by only two parameters $0 \leqslant a \leqslant 1/2$ and $1/2 \leqslant p \leqslant 1$. In Fig. 1 the distinct regions in this parameter space are displayed.

In region SC-F, i.e., for $a < 1/4$ the fractal dimension $D_0^{(2)} < 1$ and therefore a typical projection onto a line is a singular continuous measure with fractal support of dimension $D_0^{(2,1)} = D_0^{(2)}$. In regime SC-E, $1/4 < a < \min(1/2, p^2)$, one has $D_0^{(2)} > 1$, resulting in $D_0^{(2,1)} = 1$, i.e., a distribution with Euclidean support for almost all projections. Since $D_\infty^{(2)} < 1$ for these parameters, all projections are still singular. For the remaining parameter values, AC, the measure is absolutely continuous with a square-integrable density. We will show below that the projected measures are indeed of pure type as indicated, i.e., SC and AC components do not coexist for given parameter values.

In Fig. 2 we depict two typical projected densities obtained numerically in regimes (a) AC and (b) SC-E from 500 iterative construction steps and also the corresponding $f(\alpha)$ curves. These were calculated within the

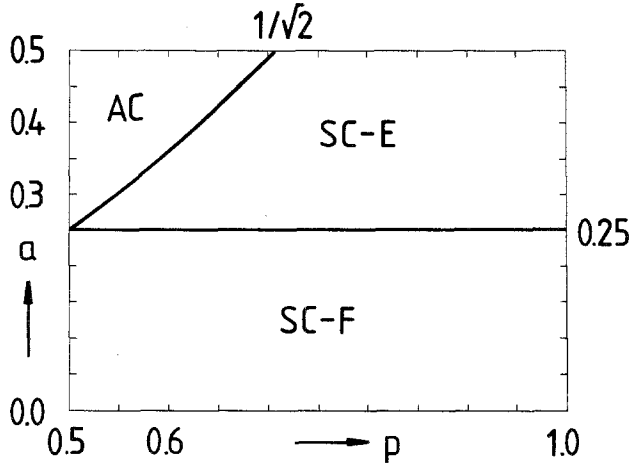

Fig. 1. The parameter space of a 2D multifractal, the product of two equal triadic Cantor measures with contraction ratio a and mass ratio p (see text), and its behavior under projections onto lines: For parameters SC-F one gets singular projected distributions with fractal support, in regime SC-E a typical projection is still singular but with Euclidean support, and for the remaining parameters (AC) one gets a square-integrable density (AC) for almost all projections.

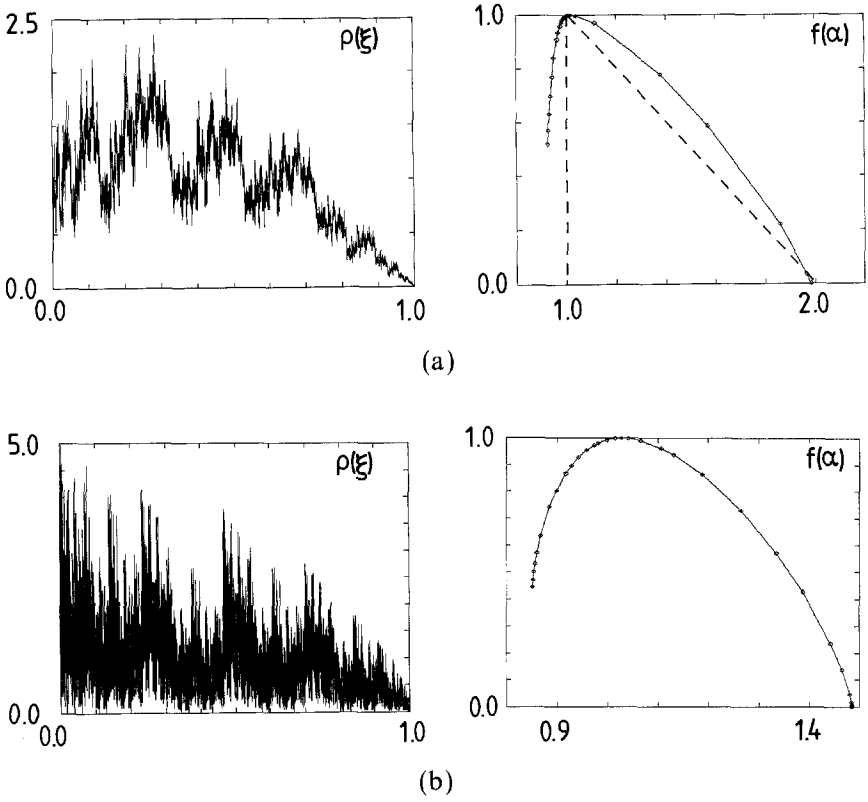

Fig. 2. (a) A density observed for a typical projection [$\mathbf{n} = (1, 0.5)$] onto a line and the corresponding $f(\alpha)$ spectrum in regime AC of Fig. 1 ($a = 0.4$, $p = 0.6$). The dashed line is the exact $f(\alpha)$ spectrum. (b) Same as (a), but in regime SC-E ($a = 0.3$, $p = 0.6$).

"canonical" formalism as described in ref. 17. From this figure one can see that it can be quite hard to distinguish numerically between the two types of behavior because in both cases the density may be quite irregular.

In Fig. 2a the exact $f(\alpha)$ spectrum is shown as a dashed line. It is well known that the divergent curvature at the maximum of the $f(\alpha)$ curve can only be inferred by extrapolating a curvature vs. resolution refinement plot[18] with the risk that a possible crossover regime is not reached. Note also that the value $\alpha_{\max} = 2$ in Fig. 2a simply reflects the power-law behavior of the density at its boundaries. We will see in the next section that the exponent of this power law depends in a simple way on the direction of the projection. By continuity this is also true for the case of Fig. 2b. Thus, in contrast to the case SC-F, where it is known that almost all projections lead to the same $f(\alpha)$ spectrum, which is identical with the original 2D

spectrum, the spectrum in region AC and SC-E is projection dependent. In the latter region, however, numerical calculations reveal a nontrivial dependence of the $f(\alpha)$ curve on the angle of projection.

The generalization of the results for projections from R^2 to R to arbitrary dimensions is also straightforward: The most singular contribution to a multifractal with Euclidean dimension N has singularity index $\alpha_{\min}^{(N)}$, which means that an iteratively constructed density $\rho_n^{(N)}$ would diverge as $a^{n\alpha_{\min}^{(N)}}/a^{nN}$ for $n \to \infty$ with $\alpha_{\min}^{(N)} < N$. To obtain a projection on a D-dimensional hyperplane one has to integrate over $N-D$ dimensions and the corresponding projected density $\rho_n^{(N,D)}$ scales as

$$\rho_n^{(N,D)} \sim \rho_n^{(N)} a^{n(N-D)} = a^{n(\alpha_{\min}^{(N)} - D)}$$

i.e., it diverges for $\alpha_{\min}^{(N)} = D_{\infty}^{(N)} < D$ (cases SC-E and SC-F) and approaches zero otherwise (case AC). Note that the assumption of a product measure is not essential in the above reasoning and we expect that these results hold quite generally. A rigorous treatment is possible so far only for projections of product measures as given in the Appendix. The latter covers, of course, many interesting situations beyond the self-similar case, such as certain self-affine measures (different contraction ratios and mass distribution ratios in each factor), products of Cantor measures with randomly shifted intervals, and/or varying contraction ratios in the construction hierarchy, etc.

For the product of N equal Cantor measures parametrized by contraction ratio a and mass ratio p the above result means that a typical

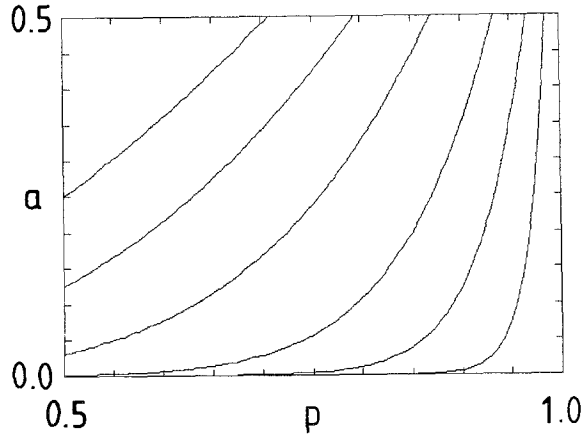

Fig. 3. The critical lines for the transition from SC-E to AC in a projection onto lines for the product of N equal Cantor measures for $N = 2, 3, 5, 10, 20, 50$ (from left to right).

projection on a hyperplane of dimension D is square-integrable if $N \log p/\log a > D$, i.e., for $a > p^{N/D}$. For projections onto lines ($D = 1$) the critical lines in parameter space for the transition from singular continuous (SC) to absolutely continuous (AC) projections are depicted for various N in Fig. 3.

This figure also illustrates the fact that the region in (a, p) space where a singular projection is obtained vanishes as N/D increases. In addition, the projected distributions also get smoother: As outlined in the Appendix, a typical projection, for example, onto a line ($D = 1$) has a square-integrable nth derivative if $\alpha_{\min}^{(N)} = \sum_{j=1}^{N} \alpha_{\min,j}^{(1)} > 2n + 1$. This is fulfilled for the product of N equal Cantor measures for $a > p^{N/(2n+1)}$.

3. CONNECTION WITH ITERATED FUNCTION SYSTEMS

The relevance of the above results for iterated function systems or linear random maps follows from the fact that self-similar Cantor measures can be regarded as invariant measures of iterated function systems of nonoverlapping construction. This implies that their projection from spaces with Euclidean dimension $N \geqslant 2$ onto subspaces with dimension D can also be regarded as invariant measures of iterated function systems in lower dimensions which are now either of nonoverlapping or of overlapping construction. The former case results in singular continuous measures with fractal support, whereas in the latter case one typically gets invariant distributions which may be singular continuous or absolutely continuous in accordance with the results depicted in Fig. 1.

To demonstrate this connection, consider the following contracting maps T_i:

$$\mathbf{x}_{t+1} = a_i \mathbf{x}_t + \mathbf{b}_i \tag{5}$$

with $i = 1,..., M$, $\mathbf{x}_t \in R^N$, and $a_i < 1$. If one randomly composes these similitudes uncorrelated and with probabilities p_i one gets an iterated function system (i.f.s.), which is known to generate a self-similar measure if a_i and $\mathbf{b}_i$ are such that one has the nonoverlapping case,[9] which, e.g., in one dimension means that the interval spanned by the fixed points of the maps T_i is mapped on disjoint intervals under one iteration of Eq. (5). A probability density $\rho_t(\mathbf{x})$ is iterated in accordance with Eq. (5) as

$$\rho_{t+1}(\mathbf{x}) = \int \left[\sum_i p_i \delta(\mathbf{x} - a_i \mathbf{x}' - \mathbf{b}_i) \right] \rho_t(\mathbf{x}')\, d\mathbf{x}' \tag{6}$$

In the nonoverlapping case the invariant density $\rho_\infty(\mathbf{x})$, respectively its integral, defines a multifractal measure with fractal support with simple

well-known expressions for $f(\alpha)$ or $D(q)$.[1-8] Projecting both sides of Eq. (6), e.g., onto lines with direction $\hat{n} \in R^N$ as in Eq. (1), one gets immediately an iteration equation for the projected density $\rho_t(\xi)$,

$$\rho_{t+1}(\xi) = \int \left[\sum_i p_i \delta(\xi - a_i \xi' - \hat{n}\mathbf{b}_i) \right] \rho_t(\xi')\, d\xi' \tag{7}$$

which is seen to define an i.f.s. in one dimension which now is of overlapping construction if $\sum_i a_i > 1$. In the limit $t \to \infty$ we get the invariant density $\rho_\infty(\xi)$ of Eq. (7), which can be interpreted as the projection of the invariant density of Eq. (6), and therefore the results of the previous section directly apply to $\rho_\infty(\xi)$. Explicitly this means that for $\sum_i a_i < 1$, Eq. (7) defines an i.f.s. in region SC-F in accordance with existing results.[19] For $\sum_i a_i > 1$ we have case SC-E or AC, depending on whether $\max_i(p_i/a_i)$ is larger or smaller than one. For the more rigorous treatment the p_i, a_i, and b_i have to fulfill certain constraints in order to be derivable from a factorizing measure in R^N: For instance, in Fig. 2 we have $a_i = a \leqslant 0.5$, $i = 1,..., 4$, $\{p_i\} = \{p^2, p(1-p), p(1-p), (1-p)^2\}$, and the $\mathbf{b}_i$ have to be located on the edges of a rectangle. The 1D maps which define, e.g., the projected density of Fig. 2b are depicted in Fig. 4. The graphs of Fig. 2 were actually calculated by exploiting this connection. The phrase "for almost all projections" in our proof translates here to "almost all shifts of the form $\xi_i \equiv \hat{n}\mathbf{b}_i$" with the $\mathbf{b}_i$ related as above.

We expect that the above results for linear maps also hold for compositions of one-dimensional nonlinear maps, like those mentioned in the

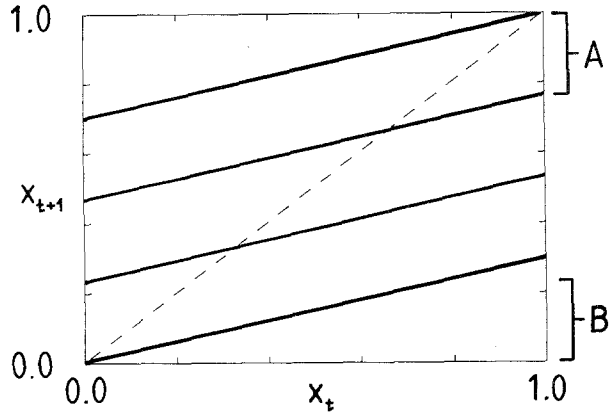

Fig. 4. The iterated function system which has as invariant density the projected distribution of Fig. 2b if the probabilities p_i are chosen as 0.36, 0.24, 0.24, and 0.16 for $i = 1,..., 4$. The asymptotic density vanishes outside the interval spanned by the fixed points of the maps (intersections with the dashed line). On intervals A and B the invariant measure is self-affine.

introduction, as long as each of them is everywhere contracting: In the same spirit as the heuristic arguments of Section 2 one should typically get square-integrable invariant densities if repeated iteration of each of the maps individually (with weight p_i) leads asymptotically to a vanishing density. In all other cases one expects singular continuous distributions which show true multifractality.

The connection with linear iterated function systems has several consequences for the original problem of projections of multifractals. First, there exists a "pure theorem"[20] for the invariant measures obtained from Eq. (7), which states that the invariant measure is either singular continuous or absolutely continuous and no mixture of these types (the pure point type occurs only in degenerate cases). Thus this theorem holds also for projections of strictly self-similar measures, which is especially meaningful in region SC-E. For more general multifractals, however, it may happen that in the latter region of parameter space a projection has in addition an absolutely continuous component. Second, there are cases, where, e.g., the four maps of Fig. 4 with slope a may be regarded as the second iteration of a two-map system with contraction ratio $a' = \sqrt{a}$. This corresponds to a special projection from $N = 2$ to $D = 1$ with direction $\hat{n} \parallel (\sqrt{a}, 1)$. For the two-map system with $a' = 1/\gamma$, with the golden mean $\gamma = (1 + \sqrt{5})/2$, and $p_1 = p_2 = 1/2$ one knows that the invariant distribution is singular continuous,[21] although the parameters of the corresponding 2D multifractal ($a = 1/\gamma^2 = 0.3819...$) lie in region AC. This means that the measure-zero exceptions of our proof are in general more complicated and not restricted to projections along the axes where the product measure factorizes. Third, since the invariant distribution of, e.g., the four-map system of Fig. 4 lies within the interval defined by the outermost fixed points, there are regions at the boundaries of this interval (denoted A and B in Fig. 4) where exact scaling relations hold, since these regions can be reached only by application of the uppermost, respectively lowest, map of Fig. 4. For case AC this means that the density, e.g., near $\xi = 0$ obeys $\rho_\infty(\xi) = (p_i/a)\,\rho_\infty(\xi/a)$, where p_i is the probability of the corresponding "boundary map." Since the maps which take this role change with the direction $\hat{n}$ and because the above scaling relation determines, e.g., $\alpha_{\max}$ of the projected density, one sees that in region AC (and also in a nontrivial manner in region SC-E) the $f(\alpha)$ spectrum depends in general on the direction of the projection.

Finally we mention an interesting aspect of the irregularity of the densities in region AC: Although the multifractal spectrum of the projected measure is trivial in this parameter region, the graphs of the invariant densities are partially self-affine (if they stem from self-similar multifractals) and can therefore also be analyzed within the multifractal formalism[22] leading to nontrivial spectra if the graphs are not differentiable. One may

speculate that one can then extract information about the original multifractal from the latter spectra, or more generally from spectra obtained from the graphs of the highest existing derivative of the densities.

4. SUMMARY

We have shown that a multifractal distribution may appear in various forms if observed in a typical projection: It may appear as an ordinary square-integrable density with trivial multifractal spectrum or as a singular distribution with Euclidean or fractal support and thus as a true multifractal. What is actually observed depends on the ratios of the generalized dimensions D_∞ and D_0 to the dimension D of the space onto which one projects. These results were obtained rigorously for projections of product measures and we gave arguments why they should hold quite generally. We also established a connection with invariant densities of iterated function systems and how the results apply there. It remains an open problem to which extent properties of the original multifractal can be inferred from a projection in cases where the Hausdorff dimension D_0 of the original multifractal exceeds D.

APPENDIX

The heuristic argument in Section 3 suggests that whenever $\alpha_{\min}^{(N)} = D(q=\infty)$ of the original multifractal increases beyond D, the dimension of the subspace on which we project, one gets an ordinary density in the projection. To prove this, consider the product of N one-dimensional measures, each characterized by a Hölder exponent $\alpha_{\min,j}^{(1)}$ resulting in $\alpha_{\min}^{(N)} = \sum_{j=1}^{N} \alpha_{\min,j}^{(1)}$ of the product. An orthogonal projection $\rho_p(\xi)$, $\xi \in R^D$, of an N-dimensional density $\rho(\mathbf{x})$, $\mathbf{x} \in R^N$, on a subspace of dimension D can be expressed by integrating over D $(N-1)$-dimensional hyperplanes with normal vectors $\mathbf{n}^{(l)} \in R^N$, $l = 1,..., D$,

$$\rho_p(\xi) = V \int d^N x\, \rho(\mathbf{x}) \prod_{l=1}^{D} \delta(\xi_l - \mathbf{n}^{(l)}\mathbf{x}) \tag{A.1}$$

where V is the D-dimensional volume spanned by the in general non-orthogonal vectors $\mathbf{n}^{(l)}$ and the ξ_l are the covariant components of ξ in the coordinate system defined by the $\mathbf{n}^{(l)}$. Similar to the case of Section 2, one projection in this representation is characterized by a continuum of equivalent $\mathbf{n}^{(l)}$, since a projection from N to D dimensions is uniquely determined by $D \cdot (N-D)$ direction cosines instead of $N \cdot D$ parameters appearing in (A.1).

The Fourier transform of Eq. (A.1) yields

$$\hat{\rho}_p(\mathbf{k}) = V \int d^N x\, \rho(\mathbf{x}) \exp\left(i \sum_{j=1}^{N} \sum_{l=1}^{D} k_l n_j^{(l)} x_j \right)$$
$$= V \prod_{j=1}^{N} \hat{\rho}_j \left(\sum_{l=1}^{D} k_l n_j^{(l)} \right) \tag{A.2}$$

with the last equality following from the assumed factorization of the density $\rho(\mathbf{x})$ into N factors $\rho_j(x_j)$. Here $\hat{\rho}$ denotes the Fourier transforms of the densities, respectively Fourier–Stieltjes transform of the measures if a density does not exist. In generalization of Eq. (3) we integrate $|\hat{\rho}_p(\mathbf{k})|^2$ over a product of N D-dimensional solid spheres in $\mathbf{n}$ space. Apart from a constant factor the resulting integral is bounded by the product of N factors of the form $I_j(\mathbf{k}) = \int_{S^D} d^D n_j\, |\hat{\rho}(\mathbf{k} \cdot \mathbf{n}_j)|^2$, $j = 1, \ldots, N$. Integrating in spherical coordinates and using the order relation for the $\varphi_j(k)$ of Eq. (4), one finds immediately that each factor

$$I_j(\mathbf{k}) \leqslant \text{const} \cdot |\mathbf{k}|^{-\alpha_{\min,j}^{(1)}}$$

This implies that

$$\int d^D k \prod_{j=1}^{N} I_j(\mathbf{k}) \leqslant c \int d^D k\, |\mathbf{k}|^{-\sum_{j=1}^{N} \alpha_{\min,j}^{(1)}} = c' \int_0^\infty dk\, k^{D-1} k^{-\sum_{j=1}^{N} \alpha_{\min,j}^{(1)}}$$

with constants c and c'. This last integral is finite if

$$D_\infty^{(N)} = \alpha_{\min}^{(N)} = \sum_{j=1}^{N} \alpha_{\min,j}^{(1)} > D \tag{A.3}$$

which is the condition for getting square-integrable densities for almost all projections onto D-dimensional subspaces of R^N.

Regarding the smoothness of projected distributions, we treat here briefly the case for projections from R^N onto lines ($D = 1$). A projected distribution has a square-integrable nth derivative if $\int k^{2n} |\hat{\rho}_p(k)|^2\, dk$ is finite. Inserting the expression (A.2) for $\hat{\rho}_p(k)$ and integrating over the N-dimensional unit cube in $\mathbf{n}$ space yields an expression which is bounded by

$$I = \int dk\, k^{2n} \prod_{j=1}^{N} \int_0^1 dn_j\, |\hat{\rho}_j(n_j k)|^2 = \int dk\, k^{2n-N} \prod_{j=1}^{N} \varphi_j(k) \tag{A.4}$$

with

$$\varphi_j(k) = \int_0^k |\hat{\rho}_j(k')|^2\, dk' = O(k^{1-\alpha_{\min,j}^{(1)}})$$

as in Eq. (4). The k integral in Eq. (A.4) can be restricted to positive values. Thus the condition $I < \infty$ yields $2n - N + \sum_{j=1}^{N} (1 - \alpha_{\min,j}^{(1)}) < -1$, or

$$D_{\infty}^{(N)} = \alpha_{\min}^{(N)} = \sum_{j=1}^{N} \alpha_{\min,j}^{(1)} > 2n + 1 \tag{A.5}$$

as condition for the square-integrability of the nth derivative of a projected distribution for almost all projections.

REFERENCES

1. H. G. E. Hentschel and I. Procaccia, *Physica* **8D**:435 (1983).
2. R. Benzi *et al.*, *J. Phys. A* **17**:3521 (1984).
3. T. C. Halsey *et al.*, *Phys. Rev. A* **33**:1141 (1986).
4. B. B. Mandelbrot, *The Fractal Geometry of Nature* (Freeman, New York, 1983).
5. T. Tél, *Z. Naturforsch.* **43a**:1154 (1988); in *Directions of Chaos*, Vol. 3, Hao Bai-lin, ed. (World Scientific, Singapore, 1990).
6. J. Feder, *Fractals* (Plenum, New York, 1988).
7. H. G. Schuster, *Deterministic Chaos*, 2nd ed. (VCH, Weinheim, 1988).
8. K. Falconer, *Fractal Geometry* (Wiley, Chichester, 1990).
9. M. F. Barnsley and S. Demko, *Proc. R. Soc. Lond. A* **399**:243 (1985); M. F. Barnsley, *Fractals Everywhere* (Academic Press, San Diego, California, 1988).
10. R. Bruinsma and G. Aeppli, *Phys. Rev. Lett.* **50**:1494 (1983); G. Györgyi and P. Ruján, *J. Phys. C* **17**:4207 (1984); S. N. Evangelou, *J. Phys. C* **20**:L511 (1984); U. Behn and V. A. Zagrebnov, *J. Stat. Phys.* **47**:939 (1987); J. Bene and P. Szépfalusy, *Phys. Rev. A* **37**:1703 (1988).
11. F. Martinelli and E. Scoppola, *J. Stat. Phys.* **50**:1021 (1988).
12. G. Radons, D. Werner, and H. G. Schuster, *Phys. Lett. A* **174**:293 (1993).
13. S. Karlin, *Pac. J. Math.* **3**:725 (1953).
14. D. Zamballa and P. Grassberger, *Complex Syst.* **2**:269 (1988).
15. P. Mattila, *Ann. Acad. Sci. Fenn. Ser. A. I. Math.* **1**:227 (1975).
16. J. P. Kahane and R. Salem, *Colloq. Math.* **6**:193 (1958).
17. A. Chhabra and R. V. Jensen, *Phys. Rev. Lett.* **62**:1327 (1989).
18. C. Godrèche and J. M. Luck, *J. Phys. A* **23**:3769 (1990).
19. K. J. Falconer, *J. Stat. Phys.* **47**:123 (1987); *Math. Proc. Camb. Phil. Soc.* **103**:339 (1988).
20. B. Jessen and A. Wintner, *Trans. Am. Math. Soc.* **38**:48 (1935).
21. P. Erdös, *Am. J. Math.* **61**:974 (1939).
22. A.-L. Barabási, P. Szépfalusy, and T. Vizsek, *Physica A* **178**:17 (1991).